Autonomous self-healing pneumatic McKibben muscle based on a new hydrogel material

A. López-Díaz[1], A. Martín-Pacheco[2], A. Naranjo[2], C. Martín[2], M. A. Herrero[2], E. Vázquez[2] and A. S. Vázquez[1‡]

March 10, 2022

Abstract

In this paper we present a hydrogel with self-healing capabilities and its application for the development of a Pneumatic Artificial Muscle (PAM). Unlike other hydrogels, our material can be used outside of aqueous environments and does not need any external stimulus to self-heal, which makes it an interesting alternative for the manufacturing of soft robots. First, the mechanical properties of the hydrogel and its self-healing ability are analyzed. Second, we present the development of a pneumatic muscle based on the classic McKibben design but including our material. Finally, we analyze the capabilities of our self-repairing muscles before and after being punctured. The results show a good performance of our actuators even after low healing periods (10 minutes).

1 Introduction

Soft robots have some characteristics that make them suitable for working with humans: they absorb impacts, they can work with fragile things and deal with unknown objects thanks to their compliance. A negative characteristic is that they are susceptible to cuts and tears which limit their use to *safe* environments. Pneumatic soft robots may also have punctures or blowouts due to overpressure.

**This work was supported by the EU 785219-Graphene Core 2 European Union (Flagship project), the Spanish Ministerio de Economía y Competitividad (project CTQ2017-88158-R), the Spanish Ministerio de Educación, Cultura y Deporte (grants FPU14/01431 and FPU17/02617) and the FEDER-Junta de Comunidades de Castilla-La Mancha (project SBPLY/ 17/180501/000204).

†1 ETSI Industriales. Universidad de Castilla-La Mancha, 13071 Ciudad Real, Spain. {antonio.ldiazcampo, andress.vazquez} @uclm.es

‡2 Instituto Regional de Investigación Científica Aplicada (IRICA). Universidad de Castilla-La Mancha, 13071 Ciudad Real, Spain. {ana.mpacheco, alicia.nchacon, cristina.mjimenez, mariaantonia.herrero, ester.vazquez} @uclm.es

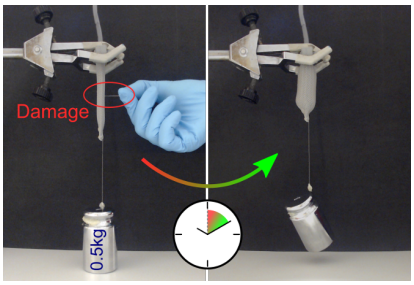

Figure 1: Self-healing McKibben muscle developed in this work. Even after a short healing time (e.g. 10 minutes), the muscle presents a good force-contraction characteristic. In the right image, the self-healed muscle lifts a load of 5 N with a contraction of 20% at 0.06 MPa actuation pressure.

This makes the search for self-healing materials one of the most active research lines in soft robotics.

Polymers are probably the most researched material in this topic. They present nice mechanical characteristic, like flexibility or deformability, but they can be damaged by high stresses, which has motivated the search of their self-healing ability. For example, in [1, 2] the authors present the development of polymeric materials that can be repaired by means of heat. Other external stimuli, such as light [3], pressure [4] or water [5], are also investigated to favor self-repair of polymers. Elastomers, which have great elastic properties (both viscosity and elasticity), are also being investigated for self-healing. For example, Cordier et al. [6] designed and synthesized a small-molecule system exhibiting rubber-like elasticity with self-healing capabilities. A comprehensive review of self-healing polymers can be found in [7].

Hydrogels are also in the spotlight due to their self-healing abilities (see [8] for a recent review). Essentially, they are networks of crosslinked hydrophilic polymers capable of absorbing and releasing large amounts of water without losing their structural integrity. They have other important properties, such as their response to external stimuli (e.g. electric fields, temperature or light [9]), which make them interesting for developing soft robotic structures, actuators and sensors. In addition, they are biocompatible and have a great resemblance to biological tissues. However, they have had a major drawback till now: they need to be immersed in an aqueous solution to work, which have limited their use in soft robots. Some examples of underwater soft robots made with hydrogels can be found in [10, 11, 12]. With the aim of taking advantage of the properties of hydrogels in any kind of environment, we have recently developed a new type of hydrogel suitable for working outside water [13]. Moreover, this hydrogel also presents good self-healing characteristics which are presented in this work together with its application in a self-healing pneumatic muscle.

Indeed, *Pneumatic Artificial Muscles* (PAM) are often used in soft robotics as, in spite of their flexibility and low weight, they can produce high forces,

absorb shocks or actively change their stiffness. These characteristics make them suitable for legged robots [14], humanoids [15] and robotic or prosthetic arms [16]. The PAM presented in this paper (see Fig. 1) is based on the *McKibben muscle* [17], which is one of the PAM designs most used in soft robotics. Our work aligns with other recent works on self-healing PAM muscles, such as the work of Terryn et al. [18], where the authors present a variant of PAM muscle named Pleated Pneumatic Artificial Muscle (PPAM) made of a Diels-Alder polymer capable of self-healing when heat is applied. Besides the use of a different material (i.e. hydrogel), our work differentiates in the way that our material does not require any external stimulus to self-heal.

Self-healing materials can also be used to develop other soft robotics structures. For example, Terryn et al. in [19] explored the use of their self-healing polymer for the construction of a soft robotic hand and a soft gripper. Other examples of self-healing materials and robots can be found in the recent survey of Bilodeau and Kramer in [20]. In this context, we are currently working on the development of other soft robotic parts with self-healing capabilities, like fingers or sensors that will be presented in future works.

The rest of this paper is organized as follows: Section 2 presents our hydrogel, its mechanical characterization and the analysis of its self-healing property. Section 3 presents the manufacturing of our McKibben muscle, its characterization and its performance after self-healing. Lastly, discussion and conclusions are presented in Section 4.

2 Hydrogel

The hydrogel used in this work is the one described previously by our research group as electroactive material [13], which is based on [2-(acryloyloxy)ethyl]-trimethylammonium chloride (AETA). The hydrogel is prepared by radical photopolymerization of AETA (56.05 wt%) as monomer, N,N'-methylenebisacrylamide (MBA, 0.08 wt%) as chemical crosslinker and sodium 2,4,6-trimethylbenzoylphosphonate (NaTPO, 0.17 wt%) as photoinitiator, using deionized water (43.70 wt%) as solvent. As described, the reaction takes place under UV light (365 nm) in 1-2 minutes, depending on the hydrogel volume and the luminous power used.

Once prepared, the hydrogels are kept under ambient conditions (25 ºC, 1 atm) for seven days. During this period, they lose water until reaching a constant weight. At this time, the hydrogels are in their equilibrated state, in which a low amount of water still remains in the hydrogel's structure. Our equilibrated hydrogels present interesting mechanical and self-healing features for being used in soft robotic applications as explained in the following subsections.

2.1 Features

The mechanical properties of our equilibrated hydrogel were characterized by compression and tensile studies in order to ascertain its stiffness and the possibility of using it in the development of PAMs. The testing machine *Mecmesin*

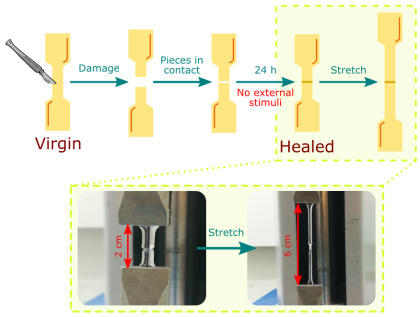

Figure 2: Procedure to prepare and analyze healed hydrogels. Virgin specimens are cut in two pieces; then, these two pieces are put in contact so that the self-healing process starts.

Multitest 2.5-i was used for this purpose.

The Young's Modulus was characterized by compression at a rate of 15 mm/min until reaching a strain of 70% of the sample initial height, obtaining a value of 457.3 ± 32.2 kPa. The energy that our hydrogels can absorb until reaching the 10% of compressive strain is 3.88 ± 0.27 kJ/m^3.

The ultimate tensile strength (UTS) and the strain to failure (STF) of the equilibrated materials were also characterized, obtaining 289 ± 111 kPa and 9.99 ± 0.51, respectively.

2.2 Self-healing ability

The self-healing ability of our equilibrated hydrogels was analyzed by tensile of both virgin and healed specimens, which are non-damaged and damaged samples, respectively.

In order to prepare the healed hydrogels, virgin specimens were firstly cut with a blade into two different pieces, and, afterwards, these two pieces were put in contact in ambient conditions for 24 hours (Fig. 2). During this time, no external forces were applied to the pieces, they were just aligned and put together at the beginning of the self-healing period. After this 24-hour period, the two pieces are rejoined, becoming a unique material again, which is named healed sample. Thus, self-healing is obtained without the necessity of any external stimulus, such as force, temperature or UV light, and without adding any healing agent.

Two values of healing efficiency (η) are obtained: one considering the absorbed energy in the linear range until 10% of strain (AE) and the other considering the fracture toughness (FT). In both cases, the efficiency is obtained by dividing the parameter of the healed specimen by the value of the virgin one ($\eta_{AE} = AE_H/AE_V$, $\eta_{FT} = FT_H/FT_V$).

Both parameters, AE and FT, were analyzed by stretching the hydrogels at 50 mm/min until their breaking point. Fig. 3 shows an example of stress-

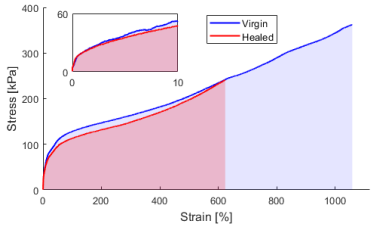

Figure 3: Tensile stress-strain curve for a virgin and a healed sample.

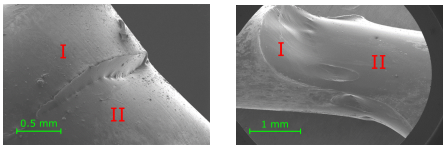

(a) Original state. (b) Stretched state.

Figure 4: SEM images of a healed hydrogel. Pieces I and II re-join to form a unique sample.

strain curves for a virgin and a healed specimen. As seen in the graph, the fracture toughness (area under the curve) of the virgin specimen is higher than the healed one, obtaining an efficiency of $\eta_{FT} = 32\%$ on average. The energy absorbed until 10% of strain is comparable in both states, leading to an average efficiency of $\eta_{AE} = 100\%$ in this linear range.

Besides, the UTS and the STF of the healed samples are 272 ± 56 kPa and 7.37 ± 1.08, respectively, showing a reduction with respect to the virgin specimens (Fig. 3). Note that, until this fracture point, the response of the healed specimen is comparable to the virgin one, which confirms a good healing efficiency.

As demonstrated, equilibrated hydrogels are capable of stimuli-free self-healing. Scanning Electron Microscopy (SEM) was performed over healed samples in order to certify this self-healing capacity. Images of a healed sample are shown in Fig. 4, in which it is possible to observe the join between both pieces, I and II. The healed sample is shown in original state (Fig. 4(a)) and in stretched state (Fig. 4(b)). This SEM study demonstrates the healing of the two pieces, which formed a unique sample after 24 hours in contact under ambient conditions.

These promising results, obtained without the requirement of external stimuli, encouraged us to apply this material in soft robotic applications as artificial muscles able to self-repair when damaged.

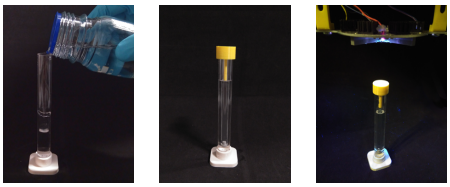

(a) Pouring the prepared solution. (b) Tube assembly with the solution inside. (c) Photopolymerization (UV light).

Figure 5: Manufacturing steps for the hydrogel-based inner bladder.

3 Autonomous self-healing McKibben muscle

3.1 Manufacture

To prove the self-healing capability of our hydrogels in a real application, we propose a hydrogel-based McKibben linear muscle. Like the traditional McKibben muscle, ours consists of an inflatable inner bladder inside a braided mesh sleeve [17]. The main difference is that our inner bladder is made of our equilibrated hydrogel.

The steps followed to manufacture this inner bladder are shown in Fig. 5. First, the solution described in Section 2 is prepared and poured into a methacrylate tube sealed at the bottom by a silicone cap (Fig. 5(a)). Then, a narrower methacrylate tube is introduced inside the solution to form the cavity of the bladder. This narrower tube is also sealed at the bottom to prevent the solution from filling it. A customized cap is 3D-printed to make these two tubes concentric (in yellow in Fig. 5(b)). Finally, the solution inside the methacrylate mold is placed under a UV light lamp (365 nm) and the bladder is photopolymerized in a couple of minutes (Fig. 5(c)).

The inner diameter of the outer methacrylate tube is 11 mm, while the outer diameter of the inner tube is 6 mm. This leads to a bladder whose walls are 2.5 mm thick when it is freshly prepared. After the formation, the bladder is exposed to ambient conditions for one week to reach the equilibrated state (see Section 2). During this water loss process, the hydrogel shrinks and the dimensions of the bladder become lower, being 2.0 ± 0.1 mm the wall thickness. The length of the bladder is controlled by the quantity of solution poured, 75 mm being the average length of the different equilibrated bladder samples.

Fig. 6 shows an example of an inner bladder next to its corresponding mesh sleeve. This sleeve is melted and wrapped up at the end corresponding to the closed end of the bladder, while the other end remains open to introduce the gas supply tube, as seen in the following subsection.

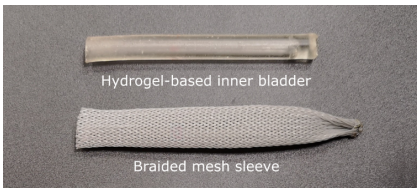

Figure 6: Components of our McKibben muscle.

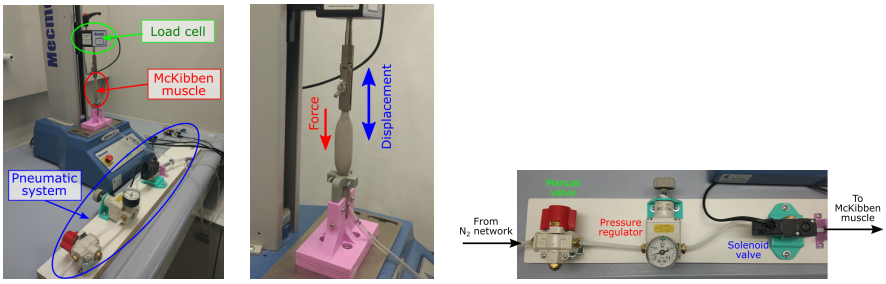

(a) Setup. (b) McKibben muscle. (c) Pneumatic system.

Figure 7: Experimental setup. The pressure in the McKibben muscle is controlled using the external pneumatic system in (c). The muscle forces and displacements are recorded by a testing machine (b).

3.2 Experimental setup

The experimental setup used to verify the performance of our muscle is shown in Fig. 7(a). The testing machine *Mecmesin Multitest 2.5-i* with a load cell rated for 500 N was used to record the force and displacement of the linear muscle, while a pneumatic system, based on nitrogen, was built to provide the muscle with the appropriate actuation.

As seen in Fig. 7(b), the muscle closed end is attached to the load cell by a claw, whereas a customized clamp was designed and 3D-printed to fix the muscle open end and the gas supply tube to the testing machine.

The pneumatic system (Fig. 7(c)) is formed by three serial components: first, a mechanical manual valve to connect our system to the nitrogen network; second, a precision pressure regulator to set the pressure inside the PAM; finally, a solenoid valve actuated by a relay controlled by an Arduino board. With this system, we were able to set pressures from 0 MPa to 0.4 MPa (4 bar) over the environmental pressure.

3.3 Characterization

Two types of procedures were analyzed to characterize our McKibben muscles:

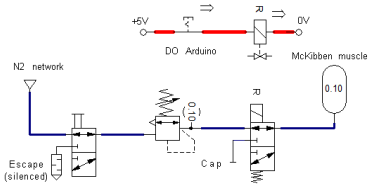

Figure 8: Schematic of the pneumatic system for the isobaric tests.

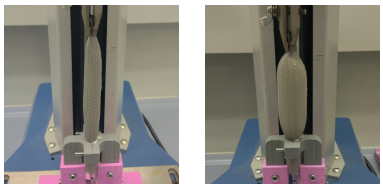

(a) Resting initial position.

(b) Maximum contraction position (null force).

Figure 9: Limit positions during the test.

3.3.1 Isobaric procedure

Designed to obtain the typical force-contraction characteristics at different constant pressures. In this procedure, both the manual and solenoid valve stay open to let the gas flow towards the muscle so that the pressure set-point is reached (Fig. 8). At any time, this pressure is guaranteed by the pressure regulator, regardless of volume changes in the muscle during the test.

The testing machine was programmed to move back and forth between the PAM resting initial length (Fig. 9(a)) and the point where the muscle exerts null force and is contracted to the maximum (Fig. 9(b)). For each pressure, several cycles were performed to reduce the Mullins effect [21], substantially present in the first 2-3 cycles.

The result of this isobaric characterization for a single virgin hydrogel-based muscle is shown in Fig. 10. The vertical axis represents the force directly measured, while the horizontal axis represents the contraction of the actuator (measured displacement divided by the actuator resting length). As commonly reported in previous works [17, 21], these McKibben muscles exhibit a hysteretic behaviour: the dashed line (lower force) corresponds to the path from the initial length to the maximum contraction point, while the solid line (higher force) corresponds to the inverse path.

This isobaric procedure was performed over virgin and punctured[1] McKibben muscles, without noticing perceptible differences between them. The reason is that the gas flow through the puncture is lower than the flow that can

[1]Details about the puncture are presented in Section 3.4.

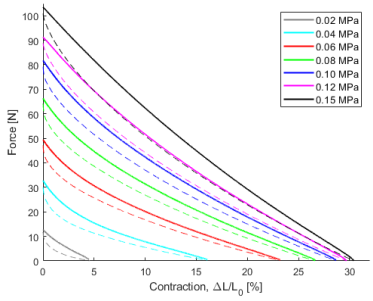

Figure 10: Experimental characteristic curves at different pressures for a virgin muscle.

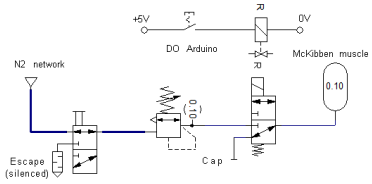

Figure 11: Schematic of the pneumatic system for the no-flow tests.

be supplied by the pneumatic system, so the damaged actuator apparently behaves in a normal manner, making this procedure not valid for the self-healing validation.

3.3.2 No-flow procedure

Designed to detect the difference between virgin and punctured muscles. In contrast to the previous case, there is no continuous input flow into the muscle: the solenoid valve is closed once the muscle is infilled with the desired pressure (Fig. 11). Since the escape of the solenoid valve is covered with a cap, the amount of gas inside the muscle should remain constant unless there is a leakage caused by damage in the muscle, making this procedure suitable for evaluating the self-healing.

Like in the isobaric procedure, several cycles are performed between the muscle initial length (no-contraction) and the maximum contraction point (null force). By contrast, the pressure inside the actuator is variable as a consequence of volume changes in the muscle. This means that the pressure inside the actuator will be lower when it is being contracted, due to its higher volume, as seen in Fig. 9(b).

An example of this behaviour for a virgin muscle is shown in Fig. 12 together with the isobaric curves for the tested pressures in grey dotted lines (colored lines in Fig. 10). As with the isobaric procedure, the muscle exhibits a hysteretic

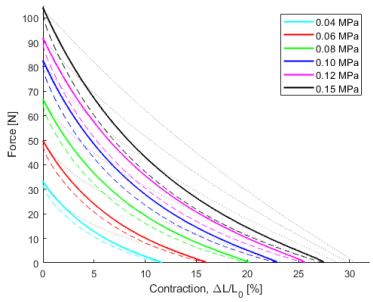

Figure 12: Experimental characteristic curves without input flow and initial different pressures for a virgin muscle. Grey dotted lines represent the isobaric curves in Fig. 10.

behaviour. Note that the force at the no-contraction point is the same as in the isobaric case, but it distances more and more from the isobaric corresponding one as the contraction increases. This is due to the decreasing pressure inside the actuator when it is contracted, as can be seen in the graph.

3.4 Self-healing validation

Based on the analysis of the two previous characterization procedures, we decided to use the *no-flow* procedure to verify the self-healing capabilities of our hydrogel-based muscle. In particular, the following sequence was carried out over seven different samples for each healing period considered:

1. Virgin muscle characterization under no-flow conditions detailed in Section 3.3.

2. Puncture on the lateral wall of the bladder. This puncture is made with a pin and a tube to hold the bladder wall during the borehole (see Fig. 13).

3. Self-healing period: the bladder is laid at ambient conditions during a specific time in which the self-healing process takes place. Three different time periods were considered: 10 minutes, 2 hours and 1 day, which is the time period used for the preliminary studies and when self-healing is proved (Section 2.2). No external stimuli or agents are applied during the whole process.

4. Self-healed muscle characterization under no-flow conditions (Section 3.3), starting with the lowest pressure and increasing it until the bladder breaks.

An example of no-flow characterization for a self-healed muscle (2 hours) is shown in Fig. 14. Grey dotted lines represent the characterization of the same muscle but in virgin state (colored lines in Fig. 12). In this case, the actuator breaks at 0.12 MPa (pink line), as can be clearly seen in the graph; the gas

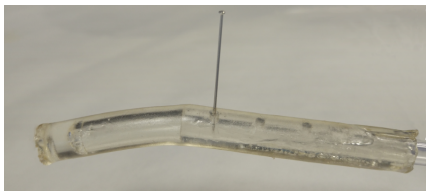

Figure 13: Puncture on the hydrogel bladder.

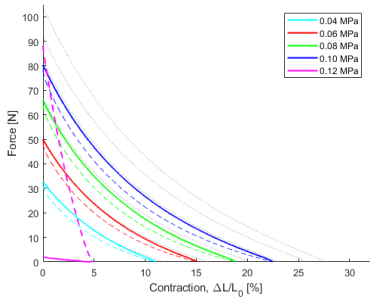

Figure 14: Experimental characteristic curves without input flow and initial different pressures for a self-healed muscle. Grey dotted lines represent the virgin muscle characteristics in Fig. 12.

escapes quickly and the pressure inside the muscle decreases sharply, leading to a zero force once the gas is fully escaped. However, until that pressure, the muscle presents an excellent actuation, replicating the execution of the virgin muscle. This fact corroborates the good healing efficiency and performance obtained in the preceding self-healing studies (Section 2.2).

In every self-healed sample tested, no matter the healing period, the actuator matches with good repeatibility the performance obtained at its virgin state. The only difference between the samples is the breaking pressure.

As was expected, the breaking pressure increases as does the healing time (Fig. 15). At 10 minutes, the average breaking pressure is 0.11 MPa, but the

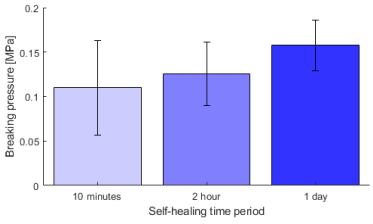

Figure 15: Breaking pressures for the different healing periods.

most remarkable aspect is that the muscle guarantees the actuation at 0.05 MPa, despite the short healing time and not adding any external agent. The breaking pressure grows to 0.125 MPa at 2 hours, guaranteeing an actuation of 0.08 MPa. Finally, after 1 day, the average breaking pressure becomes 0.157 MPa, with a guarantee of supporting 0.11 MPa. The variability between the samples at the same healing time could be due to irregularities during the manual manufacture process.

With the aforesaid method, the autonomous self-healing capability of our hydrogel-based McKibben muscle has been proved. Once healed, it is capable of repeating the same force-contraction characteristic as the virgin one until it is broken. Besides, this breaking point is assured to be greater than 0.05 MPa even after low healing periods (10 minutes).

4 Discussion and conclusions

We have presented a hydrogel material that, besides its meaningful mechanical characteristics for soft robotics, is capable of self-healing without any external stimulus. This material is proved to have a self-healing efficiency of 32% in fracture toughness and 100% in absorbed energy up to the breaking point. The McKibben muscle developed in this work benefits from both mechanical and self-healing properties, showing an adequate behavior before and after it is punctured. We have developed a *no-flow* procedure to evaluate the self-healing of punctured muscles, showing an average breaking pressure of 0.11 MPa after only 10 minutes of self-healing. The principal limitation of our work is the manual manufacturing of our muscles, which makes them irregular as shown in the variability of Fig. 15, being difficult to perform an accurate fatigue analysis. A possible solution, in which we are currently working, is the development of PAMs using 3D printing with our hydrogels.

References

[1] X. Chen, M. A. Dam, K. Ono, A. Mal, H. Shen, S. R. Nutt, K. Sheran, and F. Wudl, "A thermally re-mendable cross-linked polymeric material," *Science*, vol. 295, no. 5560, pp. 1698–1702, mar 2002.

[2] S. Zechel, R. Geitner, M. Abend, M. Siegmann, M. Enke, N. Kuhl, M. Klein, J. Vitz, S. Gräfe, B. Dietzek, M. Schmitt, J. Popp, U. S. Schubert, and M. D. Hager, "Intrinsic self-healing polymers with a high e-modulus based on dynamic reversible urea bonds," *NPG Asia Materials*, vol. 9, no. 8, pp. e420–e420, aug 2017.

[3] Y. Amamoto, H. Otsuka, A. Takahara, and K. Matyjaszewski, "Self-healing of covalently cross-linked polymers by reshuffling thiuram disulfide moieties in air under visible light," *Advanced Materials*, vol. 24, no. 29, pp. 3975–3980, jun 2012.

[4] J. Fox, J. J. Wie, B. W. Greenland, S. Burattini, W. Hayes, H. M. Colquhoun, M. E. Mackay, and S. J. Rowan, "High-strength, healable, supramolecular polymer nanocomposites," *Journal of the American Chemical Society*, vol. 134, no. 11, pp. 5362–5368, mar 2012.

[5] J.-C. Lai, J.-F. Mei, X.-Y. Jia, C.-H. Li, X.-Z. You, and Z. Bao, "A stiff and healable polymer based on dynamic-covalent boroxine bonds," *Advanced Materials*, vol. 28, no. 37, pp. 8277–8282, jul 2016.

[6] P. Cordier, F. Tournilhac, C. Soulié-Ziakovic, and L. Leibler, "Self-healing and thermoreversible rubber from supramolecular assembly," *Nature*, vol. 451, no. 7181, pp. 977–980, feb 2008.

[7] V. K. Thakur and M. R. Kessler, "Self-healing polymer nanocomposite materials: A review," *Polymer*, vol. 69, pp. 369–383, jul 2015.

[8] D. L. Taylor and M. in het Panhuis, "Self-healing hydrogels," *Advanced Materials*, vol. 28, no. 41, pp. 9060–9093, aug 2016.

[9] C. Echeverria, S. Fernandes, M. Godinho, J. Borges, and P. Soares, "Functional stimuli-responsive gels: Hydrogels and microgels," *Gels*, vol. 4, no. 2, p. 54, jun 2018.

[10] D. Han, C. Farino, C. Yang, T. Scott, D. Browe, W. Choi, J. W. Freeman, and H. Lee, "Soft robotic manipulation and locomotion with a 3d printed electroactive hydrogel," *ACS Applied Materials & Interfaces*, vol. 10, no. 21, pp. 17 512–17 518, may 2018, pMID: 29741871. [Online]. Available: https://doi.org/10.1021/acsami.8b04250

[11] M. Otake, Y. Kagami, M. Inaba, and H. Inoue, "Motion design of a starfish-shaped gel robot made of electro-active polymer gel," *Robotics and Autonomous Systems*, vol. 40, no. 2-3, pp. 185–191, aug 2002.

[12] H. Yuk, S. Lin, C. Ma, M. Takaffoli, N. X. Fang, and X. Zhao, "Hydraulic hydrogel actuators and robots optically and sonically camouflaged in water," *Nature Communications*, vol. 8, no. 1, feb 2017.

[13] A. Lopez-Diaz, A. Martin-Pacheco, R. Fernandez, A. M. Rodriguez, M. A. Herrero, E. Vazquez, and A. S. Vazquez, "A new soft fingertip based on electroactive hydrogels," in *2019 International Conference on Robotics and Automation (ICRA)*. IEEE, may 2019.

[14] B. Vanderborght, R. V. Ham, B. Verrelst, M. V. Damme, and D. Lefeber, "Overview of the lucy project: Dynamic stabilization of a biped powered by pneumatic artificial muscles," *Advanced Robotics*, vol. 22, no. 10, pp. 1027–1051, jan 2008.

[15] S. Kurumaya, K. Suzumori, H. Nabae, and S. Wakimoto, "Musculoskeletal lower-limb robot driven by multifilament muscles," *ROBOMECH Journal*, vol. 3, no. 1, sep 2016.

[16] P. Ohta, L. Valle, J. King, K. Low, J. Yi, C. G. Atkeson, and Y.-L. Park, "Design of a lightweight soft robotic arm using pneumatic artificial muscles and inflatable sleeves," *Soft Robotics*, vol. 5, no. 2, pp. 204–215, apr 2018.

[17] C.-P. Chou and B. Hannaford, "Measurement and modeling of McKibben pneumatic artificial muscles," *IEEE Transactions on Robotics and Automation*, vol. 12, no. 1, pp. 90–102, 1996.

[18] S. Terryn, J. Brancart, D. Lefeber, G. V. Assche, and B. Vanderborght, "A pneumatic artificial muscle manufactured out of self-healing polymers that can repair macroscopic damages," *IEEE Robotics and Automation Letters*, vol. 3, no. 1, pp. 16–21, jan 2018.

[19] S. Terryn, J. Brancart, D. Lefeber, G. Van Assche, and B. Vanderborght, "Self-healing soft pneumatic robots," *Science Robotics*, vol. 2, no. 9, p. eaan4268, aug 2017.

[20] R. A. Bilodeau and R. K. Kramer, "Self-healing and damage resilience for soft robotics: A review," *Frontiers in Robotics and AI*, vol. 4, oct 2017.

[21] E. G. Hocking and N. M. Wereley, "Analysis of nonlinear elastic behavior in miniature pneumatic artificial muscles," *Smart Materials and Structures*, vol. 22, no. 1, p. 014016, dec 2012.